SCIENCE CHINA
Technological Sciences

•Article•

August 2019 Vol.62 No.8: 1455–1466
https://doi.org/10.1007/s11431-018-9271-1

Cascading dam breach process simulation using a coupled modeling platform

LIU ZhiPing[1], GUO XinLei[1*], ZHOU XingBo[2], FU Hui[1], XIA QingFu[1] & LI ShaoJun[3]

[1] *State Key Laboratory of Simulation and Regulation of Water Cycle in River Basin, China Institute of Water Resources and Hydropower Research, Beijing 100038, China;*
[2] *China Renewable Energy Engineering Institute, Beijing 100120, China;*
[3] *State Key Laboratory of Geomechanics and Geotechnical Engineering, Institute of Rock and Soil Mechanics, Chinese Academy of Sciences, Wuhan 430071, China*

Received January 27, 2018; accepted April 26, 2018; published online October 10, 2018

This study evaluates the possibility of a cascade failure by developing a coupled breach-modeling platform based on one-dimensional flow modeling of the river channel, flood propagation, regulation process of reservoir fluctuation, overtopping with breaching, and wave damping downstream. A hyperbolic model of the DB-IWHR was embedded into the platform to simulate the dam breaching process. Five breach models and software were used to calculate the Tangjiashan barrier lake breaching. The results of a sensitivity study were then compared with the measured data. The peak flow and the time of occurrence were confirmed to be predictable with a reasonable accuracy if the input values were within ranges appropriate for the model. The approach was applied to a case involving two layout planning schemes for a cascade of rock-filled dams under extreme operating conditions. The probability of the failure of a key control cascade downstream caused by a continuous cascade breach upstream was simulated. Moreover, measures to prevent the transmission of risk by advance warnings were investigated. The proposed methodology and the discharge capacity measures provide guidelines to assess the risk to a cascade of dams under extreme operating conditions and offer support for the design criteria of unusual discharge structures for very large dams.

cascades, dam breach, extreme operating condition, sensitivity analysis, flood discharge structure

Citation: Liu Z P, Guo X L, Zhou X B, et al. Cascading dam breach process simulation using a coupled modeling platform. Sci China Tech Sci, 2019, 62: 1455–1466, https://doi.org/10.1007/s11431-018-9271-1

1 Introduction

The design standards for reservoirs and dams are continually being updated because of the increase in extreme global weather patterns in recent decades. The concept of probable maximum flooding or probable maximum precipitation can not meet the requirements of these new standards. The risk of disasters, such as flooding caused by dam breaches and extreme weather, should be considered in the design of groups of reservoirs formed by typical cascade development. Moreover, landslides caused by earthquakes, surges in water levels, rainfall, and melting snow can block drainage [1]. Failures of large dams have had catastrophic consequences and have drawn attention because of their importance in developing warning systems [2]. The downstream control cascade for the complex structures of flood control standards for dams and different classes of cascade reservoirs should be able to regulate the breaching flood once an upstream small reservoir is damaged and breached. The risk transmitted from the upstream cascade can be reduced to some extent. However, the breach itself causes local or global damage to the reservoir, which consequently jeopardizes the operation of the entire cascade of reservoirs mainly relying on the degree of safety of the key control cascade. With

*Corresponding author (email: guoxinlei@163.com)

improvements in the design standards used in cascade control engineering, the scale and the standard of flood discharge facilities have improved to bolster the safety of dams. Designing all flood discharge facilities based on the same standard will not be economical if the frequency of operation is not considered. The flood discharge facilities are divided into normal and abnormal facilities according to the frequency of operation to guarantee the safety of a dam. Zhou et al. [3] considered the safety of a cascade of reservoirs, and the Chinese standards for a special dam (dam with extra height) were redefined based on a quantitative analysis of breaches. Special dams were categorized into special classes 1 and 2 according to the dam height, capacity, and whether downstream reservoirs in the cascade would be affected by a breach. Class 1 refers to a dam with a height range between 250 and 300 m or a dam, whose breaching would cause a secondary break of a downstream Class 1 dam even with an early warning. Class 2 refers to a dam with a height range between 200 and 250 m, or a dam, whose breaching would cause a secondary break of a downstream Class 1 dam if an early warning is not available [4]. However, the choice of the class of dam to build to accommodate an abnormal flood discharge facility or a flood protection facility to reduce the risk of flooding remains uncertain.

A foundation in the classification of the construction of a cascade of dams is the continual estimation of a breach and consequent flooding. A single-dam breach model is the core of the hydraulic calculation of that in a cascade [3,5]. Several studies were devoted to understanding the breach process and evaluate its impact downstream and the risk of dam failure. The models proposed can be classified into parametric, simplified physical, and detailed physical models [6]. These models were used to predict the breach geometry, time of breach occurrence, and outflow [7–10]. Analytical and parametric models do not consider the physical process of breaching; hence, physical breach models feature certain hydrodynamic simplifications and assumptions. Cristofano [11] built the first analytical model for peak breach outflow, notably followed by the work of Harris and Wagner [12], Fread [13], Walder and O'Connor [14], Liang et al. [15], Wang and Bowles [16], Zhang et al. [17], Chang and Zhang [18], Erpicum et al. [19], and Wu [20], among many others. Some typical physical models, such as BRDAM [21], BREACH [13], BEED [22], and DLBreach [20], are widely used in practice. Zhong et al. [23] compared and listed some of their features. Sammen et al. [24] presented the evaluation of existing methods for the estimation of dam breach parameters using the data of more than 140 case studies of past recorded dam failures. Sattar et al. [25] developed a new empirical formula with a physical meaning using a gene expression model to predict the main breach hydrograph parameters. The reservoir shape factor, dam erodibility, and failure mode had large weights and influence on the output predictions. Zhang et al. [26] set up dynamically linked one-dimensional (1D) and two-dimensional (2D) hydrodynamic and sediment transport models for dam break flow and compared them with analytical solution. Moreover, 2D numerical models based on hydrodynamics and sediment transport equation were also developed to simulate the embankment breaching process [27]. In the recent years, HEC-RAS, MIKE11, and other well-known software were coupled with the abovementioned breach models. The dam breach mechanism involves rock and structural mechanics, hydraulic load, and geotechnical properties; hence, the overtopping flow eroding the underside of the dam, the undercutting caused by the side slope, and the horizontal, unstable collapse of the dam caused by the flow erosion process create an uncertainty in dam breach simulations [18], rendering them highly sensitive to the parameters of the hydraulic model of dam breach. To address this, Chen et al. [28] proposed a dam breach model, called the DB-IWHR, containing a calculation of the flow caused by a breach, a hyperbolic model for soil erosion from the dam, and the horizontal expansion of the breach using a numerical algorithm. This model was applied to a back-analysis of the Tangjiashan and the Hongshiyan barrier lakes [29] and effectively predicted the peak outflow and the time of failure.

The above mentioned models are available to simulate the standard configuration of the flood waves resulting from the dam failure. For a series or cascade of earth-rock dams, the probability that a downstream control cascade fails as a result of overtopping by an initial dam break depends on the effective storage, characteristic level of water, and damping of the peak wave during its propagation. These parameters are directly restricted by the discharge characteristics of the outlet structures and the pre-warning time after the breach upstream. Dewals et al. [30] developed a practical method to predict the flows generated by dam failures and malfunctions in a complex dam or a series of dams, where their simulations revealed features of primary concern for emergency planning and risk analysis. Therefore, whether the risk transmitted in a cascade upstream under extreme operating conditions can be reduced by downstream control and if some emergency measures can be implemented must be determined. This relies on the detailed and accurate prediction of the peak flow caused by the upstream dam breach, propagation of the damping wave downstream, and flood control process of the key control dam.

This study developed the platform and the procedure for a numerical simulation of a continuous breach in a cascade of reservoirs for a hazard analysis. Overtopping with breaching was modeled according to the theoretical framework of the DB-IWHR. Five breach models were used to simulate a breach in the barrier of a dam, and comparisons were made to evaluate the characteristics of each model. According to the spatial distribution of a controlled cascade of dams, the

watershed cascade studied herein was based on the cascade reservoir planning scheme for a real watershed, and can be classified into three cases, namely case I (class 1 dam-rock dam group-class 1 dam), case II (class 2 dam-rock dam group-class 1 dam), and case III (class 1 dam-rock group). Case III can be further categorized as case I. The safety problem for the cascade as a whole was investigated using the proposed platform from the perspective of the discharge safety of the key control cascade and the need to enhance the abnormal flood discharge facilities in light of such occurrences as flooding combined with a malfunctioning gate caused by an earthquake. The details and tests of the model platform and an analysis of the safety issues for the cascades of reservoirs were described in the sections that follow.

2 Cascading dam breach modeling platform

2.1 Flow modeling of the river channel

The governing equations of the dynamic wave model for open-channel flows for the flood transmission before the flooding of the reservoir and its outflow into the downstream river channel (Figure 1) are the St. Venant equations:

$$\frac{\partial A}{\partial t}+\frac{\partial Q}{\partial x}=q_1, \tag{1}$$

$$\frac{\partial}{\partial t}\left(\frac{Q}{A}\right)+\frac{\partial}{\partial x}\left(\frac{\beta Q^2}{2A^2}\right)+g\frac{\partial h}{\partial x}+g(S_f-S_0)=0, \tag{2}$$

where x and t are the spatial and temporal axes, respectively; A is the sectional flow area of the river channel; Q is the flow discharge; h is the flow depth; q_l is the side discharge per unit channel length; g is the gravitational acceleration; β is a correction coefficient for the momentum caused by the nonuniformity of the velocity distribution at the cross-section; S_0 is the bed slope; and S_f is the friction slope defined as $S_f=Q|Q|/K^2$, where K is the conveyance.

Research on the solution of the abovementioned equations is mature. The Newton-Raphson method was used herein to linearize the equations, and the most widely used implicit four-point finite difference scheme first proposed by Preissmann was applied to obtain an iterative solution.

2.2 Flood regulation process of the reservoir

The bottom elevation of the incoming flow to the river channel and the intersection of the reservoir for the upstream reservoir shown in Figure 1 were equal. The boundary conditions then satisfied the following relations:

$$h_n=h_s, \tag{3}$$

$$\frac{dW}{dh_s}\frac{dh_s}{dt}=Q_{in}(t)-Q_{out}(z,m), \tag{4}$$

where $Q_{in}(t)$ is the inflow corresponding to the upstream flood wave reaching the reservoir; $Q_{out}(z,m)$ is the outflow of the reservoir at t; the flow before dam breach is the discharge flow of the outlet structure; and m is the discharge coefficient of the outlet structure. If the dam is breached, the outflow is the sum of the discharge flow from the outlet structure and the outflows caused by crest overtopping and breaches:

$$Q_{out}(z,m)=C_sL_s(z-z_s)^{1.5}+C_gA_g(z-z_g)^{0.5}+Q_y+Q_b, \tag{5}$$

$$Q_b=CB\left[\max(z-z_d,0)\right]^{1.5}, \tag{6}$$

where Q_y is the term for diversion or pumping flow uncorrelated with the water head; Q_b is the flow caused by the dam breach; and C_s, C_g, and C are the discharge coefficients of the non-pressure spillway, gated flood discharge tunnel, and dam breach, respectively. L_s is the width of the spillway; A_g is the area of the open gate; and C is the discharge coefficient with the theoretical value of 1.7 $m^{1/2}/s$. Researchers used values of C ranging from 1.3 to 1.7, and many used a lumped coefficient for C in their calculations [12,18]. z_s, z_g, and z_d are the elevations of the uncontrolled tunnel, gated flood discharge tunnel, and weir crest of the dam, respectively.

2.3 Overtopping and dam breach modeling

When overstandard flood flow upstream enters into the reservoir, the water level goes through three stages, namely water rise, overtopping, and breaching, if the dam is expected to fail or be breached as a result of the overtopping flow. The type of failure and the corresponding breach parameters must be determined. The bottom of the crest channel begins scouring if the flow velocity of the crest in the dam further increases to a certain incipient velocity V_c. The dam breach process then begins [28]. The dam breach flow given by eq. (6) should be equal to the loss in the reservoir's water storage shown as follows [31,32]:

$$Q_b=CB(z-z_d)^{1.5}=\frac{dW}{dz}\frac{dz}{dt}+Q_{in}-q, \tag{7}$$

where q is the reservoir's outflow, excluding the dam breach flow, and W is the reservoir's water storage capacity considered as a function of water level z. The relationship between storage and water level can be found in Liu et al. [33] and approximated by

$$W=\left[p_1(z-H_r)^2+p_2(z-H_r)+p_3\right]\times 10^6,$$

where H_r is the reference water level.

Δz is measured from time t to $t+\Delta t$ to ensure that the increment in z is always positive in the calculations:

$$\Delta z=z(t)-z(t+\Delta t). \tag{8}$$

When the flow velocity at the crest of the dam is less than V_c, eq. (7) for the increment in the reservoir can be solved based on the following difference equation once the abovementioned balance equation has been differentiated:

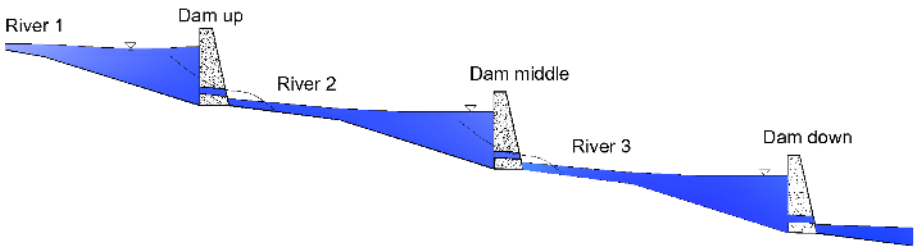

Figure 1 (Color online) Layout of the cascade earth-rock dams considered in the study.

$$CB(z-z_{\mathrm{d}}+0.5\Delta z)^{1.5}=\frac{\mathrm{d}W}{\mathrm{d}z}\frac{\mathrm{d}z}{\mathrm{d}t}+Q_{\mathrm{in}}-q. \tag{9}$$

We obtain the following when Δz is small:

$$(z-z_{\mathrm{d}}+0.5\Delta z)^{1.5}\approx(z-z_{d})^{1.5}+0.75\Delta z(z-z_{\mathrm{d}})^{0.5}. \tag{10}$$

Substituting eq. (10) into eq. (9) yields:

$$\Delta z=\frac{\left[Q_{\mathrm{in}}-q-CB(z-z_{\mathrm{d}})^{1.5}\right]\Delta t}{\left[\frac{\mathrm{d}W}{\mathrm{d}z}+0.75CB(z-z_{\mathrm{d}})^{0.5}\Delta t\right]}. \tag{11}$$

The erosion caused by the breach and its horizontal expansion is considered if the flow velocity at the crest of the dam is higher than V_{c}, where the hyperbolic model of the DB-IWHR proposed by Chen et al. [28] can be used to simulate the rate of erosion caused by the breach:

$$z'=\Phi(\tau)=\frac{\upsilon}{a+b\upsilon}, \tag{12}$$

$$\upsilon=k(\tau-\tau_{\mathrm{c}}), \tag{13}$$

where υ is the shear stress with reference to its critical component; a and b are coefficients either regressed from the test results or based on experience; k is the unit conversion factor that allows z' to approach its asymptotic value within the working range of τ; and τ_{c} is the incipient shear stress.

Widely accepted rigorous analytical methods with circular slip surfaces, such as Bishop's simplified method, are applied for the lateral enlargement modeling. The conventional discrete method [13,18] initiates the calculation from a given initial time t_0 with time step Δt to determine the corresponding water level increment ΔH, scouring depth Δz_s, and flow velocity variation ΔV. The new approach proposed by Chen et al. [28] was the first to provide the initial flow velocity V_0 and the flow velocity increment ΔV to solve the corresponding ΔH, Δz, and Δt.

2.4 Framework of the modeling platform

Note that after the overtopping of the water level, the calculation will turn to the dam breach mode when dam breach scouring reaches the incipient velocity V_{c}. A cascading dam breach is a key point of this platform and more different from a single dam breach, in which the breaching flood from the upstream dam may cause some amplification effects in the breach flood of the downstream dam. Some empirical models feature certain hydrodynamic simplifications and assumptions that can be used to predict the time of breach occurrence and outflow rate, but do not consider the physical process of breaching. The modeling of the breaching process and the peak discharge are both important because they affect the estimation of the flood wave propagation and the inundation process. Therefore, when we calculate the breach in the middle reservoir, the propagated flow as a result of overtopping by the initial breach (upstream dam) should overlap with the inflow of the reservoir (Q_{in} in eq. (9)) for the calculation when the water level reaches the crest of the middle dam. The dam breach flow process overlaps with that of river 2 for the next stage in the upstream reservoir, for which the evolution, middle reservoir fluctuation, and continuous breach process are repeated for the three steps mentioned earlier. The platform was developed using the C programming language and its framework shown in Figure 2 depicts how the platform works.

3 Comparative analysis of the dam breach models

The HEC-RAS, MIKE11, DAMBRK, BREACH, and the abovementioned numerical platforms based on the DB-IWHR were used to evaluate the reliability and the difference between the model and commercial software, simulate the Tangjiashan breach process, and compare the results with the measured data. The input parameters, such as natural inflow, initial breach width, and reservoir water storage, were similar to those in Chen et al. [28]. The incipient velocity V_{c}, at which soil erosion commenced for Tangjiashan, was approximately 2.6 m/s.

Figure 3 shows the flow of water through the breach and other information of the breaching process calculated by the abovementioned model. The figure and the debugging calculation clearly showed that the peak discharges and the arrival times calculated by the Mike11 DB and HEC-RAS models were close to the measured value, but with the condition that the initial and final sizes and the development of the breach were preset; otherwise, the measured difference would have been very large. The trends of the flow and the variation in the water level calculated by the DAMBREAK

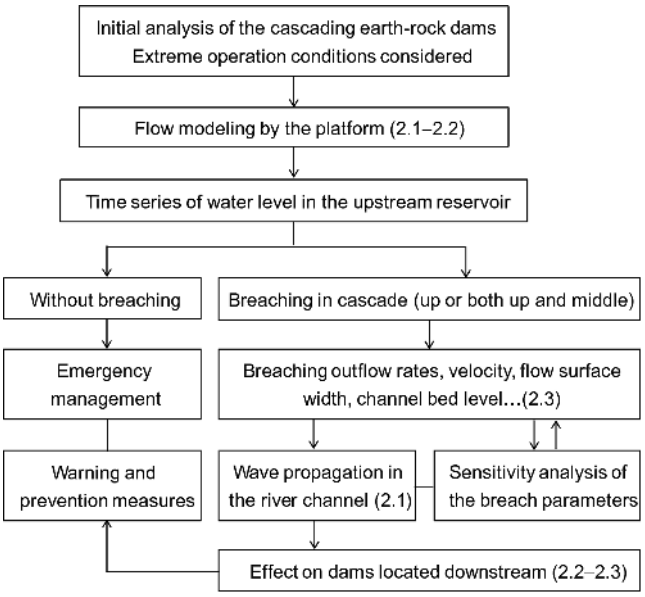

Figure 2 Framework of the cascading dam breach modeling platform.

model were consistent with the actual results. However, the breach duration, initial and final sizes of similar breaches, and their expansion should also be entered. These parameters were unknown. The sediment transport, stability of the slope of the dam breach, and other factors were considered in the BREACH model to calculate the complete breach process. Moreover, the flow consistency was adequate, but numerous uncertain parameters existed in the model. The parameter sensitivity was also strong, and the presumed ratio of the section width of the dam breach to depth in the model lacked a theoretical basis. The difference between the measured and calculated values of the breach size was large. The influence of the geometrical parameters, material properties, and initial condition of the breach was considered in the DB-IWHR model. With reference to the measured data for the Tangjiashan and Hongshiyan barrier lakes [29], a set of parameters (i.e., a=1.1, b=0.0007, and τ_c=30 Pa) was used because they were close to the field measurements at an erosion rate of 1.19 mm/s. The predicted peak discharge was 7470 m^3/s compared with the measured value of 6500 m^3/s. Other characteristic values, such as time of occurrence and water level, agreed with the measured data before the peak flow. The calculated elevations in the water in the reservoir and the channel bed continued to decrease, while the measured data remained almost unchanged. This shortage can be explained by the sedimentation of a large amount of scoured material in the downstream riverbed after the peak outflow. However, compared with the other models, parameters, such as the dam breach size, were not needed as known conditions to enter, which was more significant in forecasting dam breaches. A sensitivity study on the BREACH, Mike11 DB, and DB-IWHR models was also conducted for this case by changing a typical model parameter each time while keeping

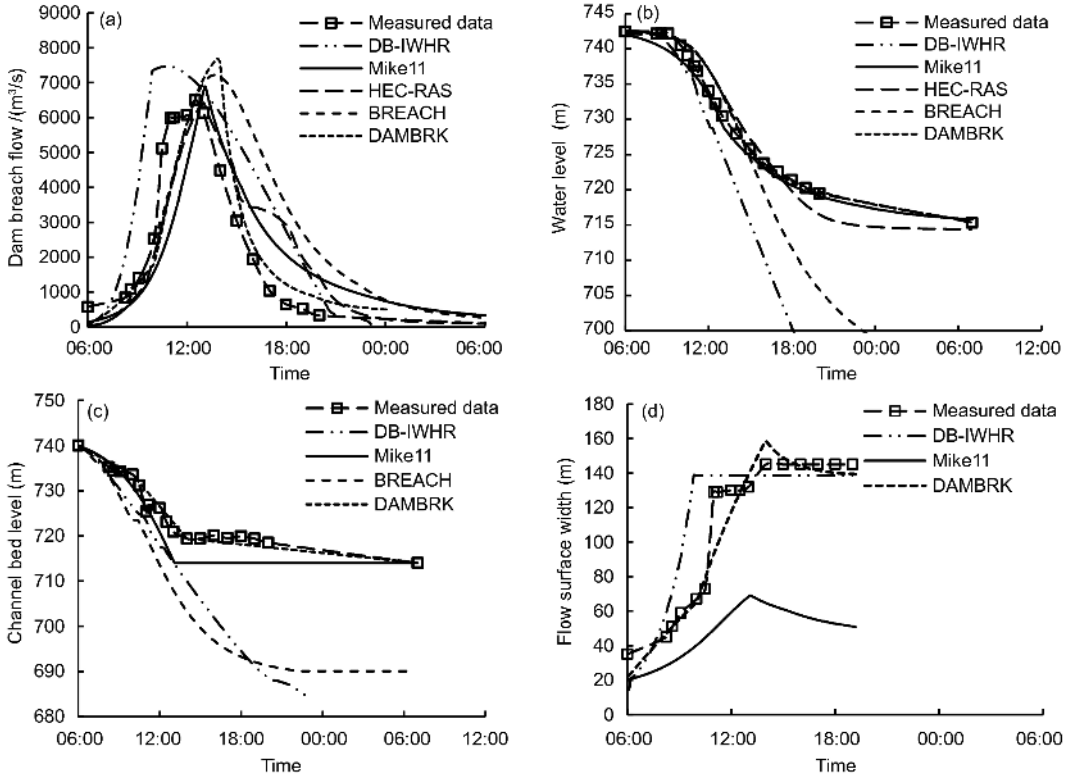

Figure 3 Comparison of dam breach models. (a) Dam breach flow; (b) water level of the reservoir; (c) channel bed level; (d) flow surface width.

the others constant. The back-analysis results shown in Table 1 confirmed that the peak flow and the time of occurrence can be predicted with a reasonable accuracy if the input values are carefully selected. The percentage error of the peak flow prediction by the hyperbolic model was smaller than that of the other models. It could handle a wide range of parameter inputs, and was especially less sensitive to the input of the erosion parameters. Considering the dam breach and the peak time of flooding of the reservoir under extreme conditions, the DB-IWHR model was easy to apply and robust and, hence, had a significant potential for application.

The abovementioned models and platforms were used to calculate and analyze the discharge safety issues for the cascade as detailed below.

4 Application and case study

This case referred to the planning scheme of a watershed in the southwest of China (Figure 4). The dams in cascade of Xiazhuang, Bagou, Dali, Bushi, and Shuangtunzi were used, where Bagou, Dali, and Bushi were small earth-rock dams with a regulated storage capacity of 0.07, 1.506, and 0.19 hundred million m^3, respectively. The concrete-face rock-filled dams Xiazhuang and Shuangtunzi formed the key control cascade with higher storage capacities. Table 2 shows the typical parameters of the reservoirs. For convenience of study and comparison, classes 1 and 2 (Xiazhuang I and Xiazhuang II, the dam height and storage were different, but corresponded to the same hydrograph of storage capacity) were considered for the trial design of the control reservoir in the upstream Xiazhuang. The regulated storage capacity was small; hence, the sum of the storage capacities of the earth-rock dam group was temporarily considered equivalent to that of the Dali reservoir. The regressions on the parameters of the erosion rate of the dam based on the measured data were performed with a=1.1 and b=0.001 in eq. (10), which were different from the barrier lake. The mountainous rivers 2 and 3 in Figure 1 were processed as inverted trapezoids, where the slope, width, slope coefficient, and manning roughness coefficient of the river were 0.004, 30 m, 0.3, and 0.025, respectively.

4.1 Case I (class 1 dam-rock dam group-class 1 dam)

When the Xiazhuang reservoir was considered to belong to special class 1 (Xiazhuang I), this cascade was a typical up-and-down comparative. Table 1 shows that the regulated

Table 1 Sensitivity analysis results

Model	Typical parameter	Values	Occurring time of peak flow	Peak flow (m^3/s)
BREACH	Porosity	0.2	15:29	4982.8
		0.4	13:41	7217.5
		0.6	12:07	10686.9
	Grain size distribution uniformity d_{90}/d_{30}	10	15:04	5582.5
		30	13:41	7217.5
		50	13:43	8115.4
	Internal friction angle φ (°)	15	13:17	7401.8
		22	13:41	7217.5
		35	14:25	6700.5
Mike11 DB	Porosity	0.2	16:26	5403.7
		0.4	13:06	6822.1
		0.6	10:50	8234.4
	Initial width of breach	8	13:36	6455.6
		14	13:06	6822.1
		20	12:50	7278.3
	Lateral erosion rate	0.12	13:10	6487.5
		0.2	13:06	6822.1
		0.3	13:00	7414.7
DB-IWHR	Drop coefficient $m=h/(H-z)$	m=0.8	10:51	7470.0
		m=0.7	10:54	7688.6
		m=0.6	10:51	7828.6
	Erosion rate parameters	a =1.1 b = 0.0007	10:51	7470.0
		a =1.0 b = 0.0006	10:40	8457.8
		a = 0.9 b =0.0005	10:37	9705.6

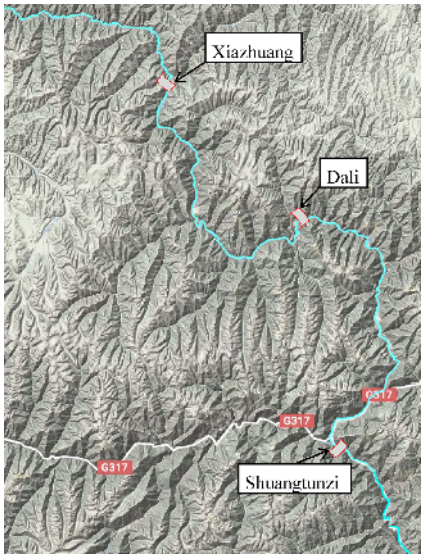

Figure 4 (Color online) Layout of the three dams considered in the case study.

storage capacity of Xiazhuang was 1924 million m^3. In case of its breach, the capacity of the dam group Dali was limited and, hence, not cut-off flooding caused by the breach. Based on a past work [5], the breach will occur after a breach in a special class 1 dam, regardless of whether the pre-warning was valid in the downstream class 1 dam. Therefore, from the perspective of discharge safety, this layout should ensure that the up-and-down dam must not be breached, which means that the break should not occur in the Xiazhuang reservoir under any condition. A spillway, a deep-hole flood discharge tunnel, and an emptying tunnel were set for the outlet structure design of Xiazhuang. The working head was high because the bottom elevation was low. Moreover, the conditions were poor for the flood discharge of the emptying tunnel, such that it was not involved. This was intended to analyze extreme operating conditions (i.e., overstandard flooding combined with a gate being rendered inoperative by an earthquake) and the discharge safety in light of the need to augment the overflooding facilities of the Xiazhuang class 1 dam.

The magnitude of overstandard flooding was temporarily considered based on the probable maximum flooding (PMF), which refers to a once-in-10000-years flood plus 20%. When overstandard flooding occurred, the flood was discharged through a gate from the outlet structure. In the case of an earthquake that damaged a discharge gate and caused it to become inoperative, the total discharge capacity of the outlet structure was reduced. This reduction was temporarily considered to be 10%–20%. The reservoir would then be regulated at a normal water level of 3120 m (adverse water level). The typical characteristic values of the once-in–10000 years flood and the PMF were used. Figure 5 presents the flood hygrograph. The flood had two peak processes, where the flood was up to 4990 m^3/s for 10 h and from 4160 m^3/s to 4990 m^3/s for approximately 1 h. Figure 6 depicts the water level fluctuation under a different flood regulation scheme based on eq. (4) in Xiazhuang I. The reservoir flooding under these conditions was regulated from the beginning through a gate. The corresponding discharge capacity was over 3000 m^3/s. The incoming flow in the first 4 h was less than the discharge capacity, and the water level of the reservoir first fell by 0.3 m after rising. The flood discharge then instantly increased. Accordingly, the water level of the reservoir was immediately banked up. The water level of the reservoir fell in amplitude and continued rising before and after the second flood peak. The discharge capacity of the gate was subsequently greater than the flood discharge, and the water level decreased. The total incoming flood volume at approximately hour 54 of the process was 753 million m^3, and the water level of the reservoir reached a peak value of

Table 2 Typical parameters of the earth-rock dam cascades

Item	Xiazhuang I	Xiazhuang II	Dali	Shuangtunzi
Elevation of crest (m)	3126	3070	2690	2510
Max. dam height (m)	231	175	113.5	314
Max. flood level (m)	3122.87	3065	2687.61	2504.42
Normal flood level (m)	3120	3062	2686	2500
Elevation of dead water (m)	3060	3010	2683	2420
Total reservoir storage (hundred million m^3)	30.19	10.9	1.85	28.97
Normal reservoir storage (hundred million m^3)	29.05	10.24	1.766	27.32
Dead storage (hundred million m^3)	9.81	2.7	1.606	8.15
Natural inflow (m^3/s)	185	185	206	516
Distance (km)	0	0	85.6	174.9
p_1	0.207	0.06	0.04	0.16
p_1	19.65	-4.74	4.94	11.07
p_1	981.13	90.19	161.49	814.65
Reference water level	3060	2895	2683	2420

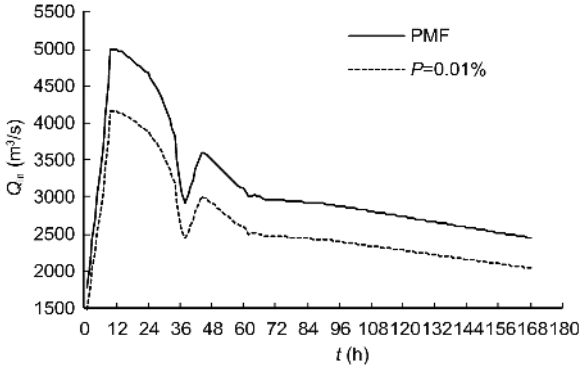

Figure 5 Flood hydrograph of the Xiazhuang I reservoir.

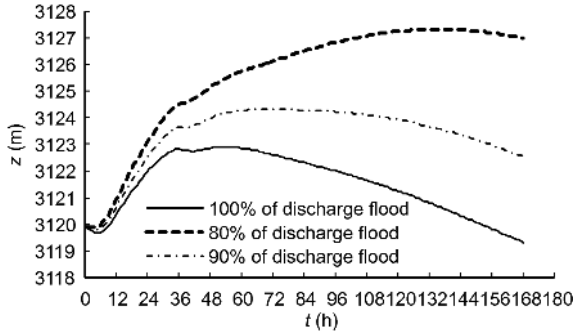

Figure 6 Fluctuation in the water level under different flood regulation schemes.

3122.92 m, which was 3.08 m from the dam crest of the reservoir. The peak value of this water level was close to the maximum flood level (3122.87 m), indicating that the overstandard flooding conditions were sufficiently considered in the original design, and a margin was maintained. The discharge capacity of the outlet structure decreased when a discharge gate was damaged by an earthquake. Moreover, the water level of the reservoir was at 80% and 90% of the regulated flooding discharge (Figure 6). The peak value of the banked-up water level of the reservoir rose to 3124.31 m in hour 71 of the flood process when 10% of the discharge capacity was lost because of an inoperative gate. The discharge capacity was subsequently greater than the incoming flow, and the water level fell. In this process, the peak water level was still 1.69 m from the dam crest, but safety was strengthened only, such that it did not result in a breach. The peak banked-up water level of the reservoir was up to 3126.02 m by hour 69 of the overstandard flooding process, which was over the crest of the dam, when the gate was inoperative. The lost discharge capacity was 20% of the total capacity. The reservoir was overtopping, which provided an opportunity for setting an abnormal flood discharge facility to reduce the risk of the flood discharge. The growth rates dz/dt (by the hour) for the water level of the reservoir for the three abovementioned working conditions in the first peak discharge time were 0.12, 0.15 and 0.17 m/h, respectively. Compared with the growth rate of 80% in the water level-given discharge capacity, the rise in the water level was 0.05 m/h lower when the discharge gates were working, indicating that the abnormal overflow discharge facility could effectively eliminate the rise in the water level when the discharge gate was invalid.

The results showed that the reservoir would have dam overtopping and breach problems if the extreme working conditions of the overstandard flooding with an inoperative gate were considered. The class 1 dam in this case must enhance the abnormal overflow facilities to better deal with the situation. Under circumstances, where part of the upstream overstandard flooding and the normal flood discharge facilities have broken down, the reservoir capacity of the dam would be relieved by a timely discharge and would be protected from breaches. The specific magnitudes can be determined through the method and the calculation in this study. Using this case as an example, the discharge capacity of the abnormal overflow facilities must be 20% of the original overflow weir and the deep-hole flood discharge tunnel. The starting conditions of which can be determined according to the failure condition of the gate and the forecasted or monitored peak discharge and time.

4.2 Case II (class 2 dam-rock dam group-class 1 dam)

The total storage capacity of the Xiazhuang reservoir in the abovementioned case was reduced to 1024 million m^3. Hence, it was reclassified as a class 2 dam. Its special layout pattern was that in case II. According to the conditions laid out in the definition of special class 2, this dam was a special class 2 after the breach, a continuous breach when the prewarning was invalid, and no breach when it was valid in the downstream special class 1 dam. This cascade was assumed to be operated under extreme conditions, implying that a breach occurred in Xiazhuang II. The flood wave propagation in the downstream river and the possible dam breach of the special class 1 Shuangtunzi reservoir were simulated.

4.2.1 Dam breach and flood propagation at Xiazhuang II

Xiazhuang II suffered from extreme overstandard flooding, and a breach occurred at time 0. The incipient velocity of the dam was 3 m/s. The flood calculated by the method described in sect. 2.3 reached a peak discharge of 15000 m^3/s at hour 10.7. The water level subsequently decreased, and the flow reduced. The dam breach lasted for approximately 40 h. In the calculation, the timer shaft was counted from 0. Dali is 85.6 km from the Xiazhuang II reservoir, and the difference in the altitude between them was 318 m. Based on the method in sect. 2.1, the 1D evolution model θ of the flood was 0.6, and the time step was 60 s. Figure 7 shows the breach process and the flooding evolution of the reservoirs. The flooding caused by the breach evolved in the Dali re-

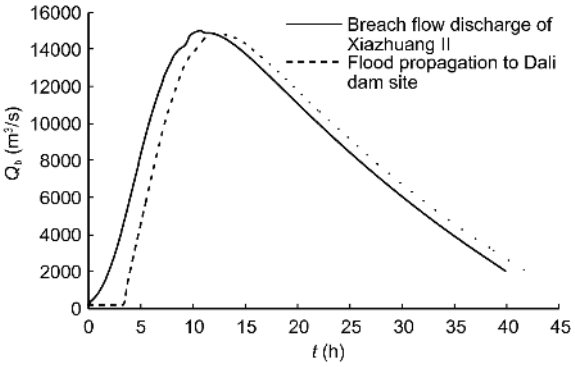

Figure 7 Dam breach for the failure of Xiazhuang II and flood propagation to the Dali dam.

servoir after 3.25 h, and the peak discharge was 14797 m^3/s at hour 12.3 without a notable decrease.

4.2.2 Continuous cascade breach at Dali and flood propagation

According to the calculation method in sects. 2.2 and 2.3, the water level of the reservoir at Dali rose to the dam crest at hour 5.32 (Figure 8). The peak discharge of the incoming flow was large; hence, the overtopping overflow of the Dali reservoir was smaller than the incoming flow. Furthermore, the water level of the reservoir continued to rise. The banked-up height of the water level when the overtopping flow velocity reached V_c of the breach scour was calculated by adding the Dali continuous breach. The Dali reservoir reached a continuous breach peak discharge of 23513 m^3/s at hour 14.6, and the breached lasted for 21.5 h. Flooding continued to evolve to downstream Shuangtunzi after the breach of the Dali reservoir. The distance between the reservoirs was 89.3 km, while the difference in altitude was 380.5 m. The flooding arrived at the Shuangtunzi at hour 8.7. The flood peak occurred at hour 15.95. Figure 9 shows the continuous breach process and flood propagation.

4.2.3 Discharge without pre-warning in Shuangtunzi

The outlet structures of Shuangtunzi included a spillway, a vertical shaft discharge tunnel, and a deep-hole flood discharge tunnel. The discharge flow was up to 6819.6 m^3/s when the total discharge was at a water level of 2500 m. The continuous breach flooding entered the dam site at the Shuangtunzi reservoir at hour 8.7. No pre-warning was observed in this reservoir; hence, the flood was discharged at all gates when the dam breach from Dali entered it. The water level of the reservoir rose to the dam crest at an elevation of 2510 m at hour 19.5 and rose to 2511.2 m (top elevation of the wave wall) at hour 20.9 because the discharge was fast. The dam was overtopping, and the water level rose to its highest level at 2513.29 m in hour 25.7. Figure 10 presents the inflow, discharge outflow, and variation in the water level.

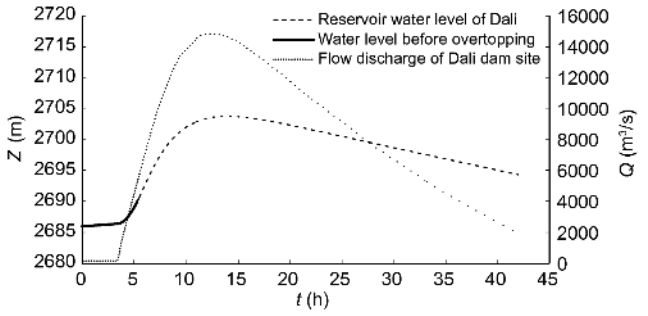

Figure 8 Flooding and water level of the reservoir of Dali after the Xiazhuang II failure.

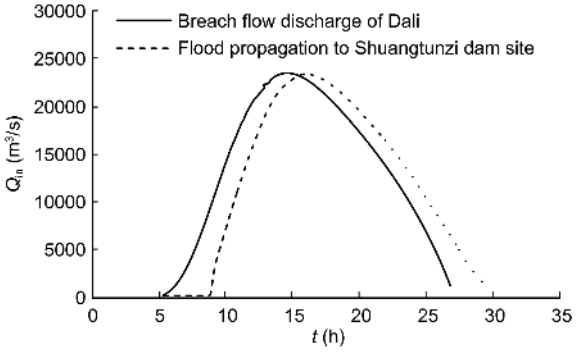

Figure 9 Dam breach for the continuous failure of Dali and flood propagation to the Shuangtunzi dam site.

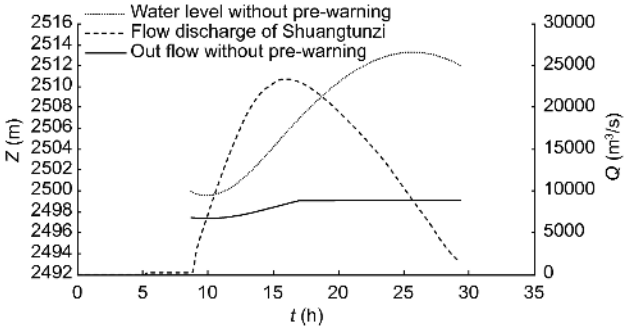

Figure 10 Inflow, outflow, and flood regulation process of Shuangtunzi without pre-warning for the upstream cascade breaches.

4.2.4 Discharge with pre-warning in Shuangtunzi

The flooding from Shuangtunzi was discharged from all gates at a water level of 2500 m when the upstream Xiazhuang II was breached. Figure 11 illustrates the water level. The continuous breach flooding of Dali took 8.7 h to propagate to the Shuangtunzi reservoir. The water level of Shuangtunzi already decreased to 2494.75 m, and the amplitude of the reduction was 5.25 m, indicating that a part of the storage capacity was emptied out in advance. The dam breach flooding flow was subsequently smaller than the discharge capacity of the outlet structure. Moreover, the water level of the reservoir was further reduced to its lowest

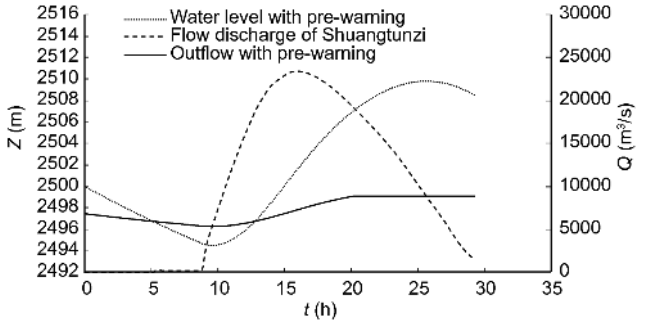

Figure 11 Inflow, outflow, and flood regulation process of Shuangtunzi with pre-warning for the upstream cascade breaches.

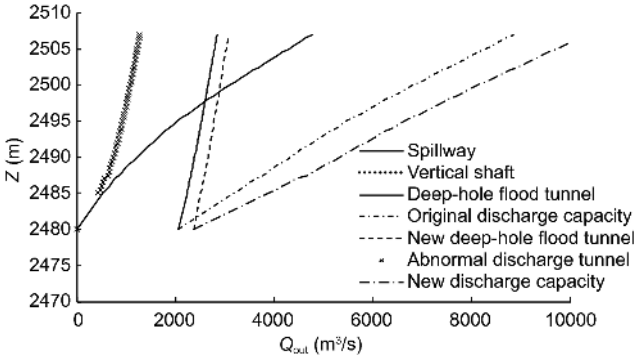

Figure 12 Outlet structure discharge curve of Shuangtunzi.

level of 2494.50 m at hour 9.7. At this time, the inflow was equal to the outflow. The flood discharge was subsequently greater than the water discharge from the entire outlet structure. In addition, the water level of the reservoir started rising. The water level rose to 2509.79 m when the inflow was equal to the outflow at hour 25.6 for the second time. This value was 0.21 m lower than the crest elevation and 1.41 m lower than the crest elevation of the parapet wall of the dam. The simulated results showed that this class 1 dam was not breached under a continuous cascade breach upstream because the flood regulation storage capacity was increased for all the gate discharges with pre-warning in Shuangtunzi. However, the margin of safety was very low.

4.2.5 Increased discharge capacity without pre-warning

Under this condition, the discharge capacity was increased for Shuangtunzi compared to the original. The capacity of an abnormal flood discharge tunnel was increased, with the scale of flood discharge comparable to that of the vertical shaft. Measures were taken to reduce the inlet elevation of the existing deep-hole flood discharge tunnel (temporarily by 10 m). The discharge capacity increment of the single deep-hole flood discharge tunnel at water levels above 2500 m was in the range of 8.42%–9.45% when the deep-hole bottom elevation was reduced. The total discharge capacity increased by 16.8%–19.1% compared with the original discharge capacity. Figure 12 presents the flood discharge curve.

The continuous flooding of Dali was immediately discharged through all the gates after it entered the dam site of the Shuangtunzi reservoir at hour 8.7. The flood propagation flow increased too quickly; hence, the water level of this reservoir rose to a crest elevation of 2510 m at hour 21.2 and 2511.2 m at hour 24. The dam then started to overtop. The water level rose to its highest elevation of 2511.31 m after hour 25. Figure 13 shows the entire inflow, discharge outflow, and variation in the water level. Compared with the discharge capacity of Shuangtunzi without pre-warning, the water level of Shuangtunzi rose slowly under the condition of the same upstream continuous flooding as the discharge

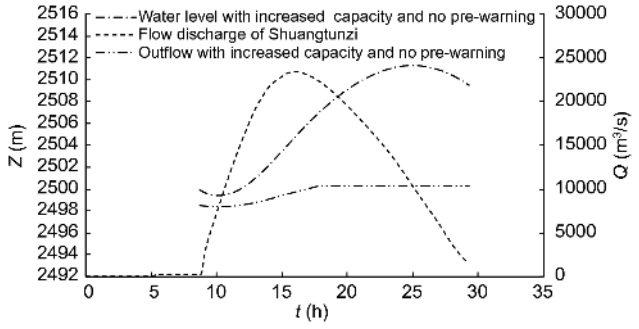

Figure 13 Inflow, outflow, and flood regulation process of Shuangtunzi with an increased discharge capacity, but no pre-warning of the upstream cascade breaches.

capacity increased. However, it finally overtopped. The pre-warning time of the dam breach was very significant for control cascade discharge safety when dams were arranged in series.

4.2.6 Increased discharge capacity with pre-warning

Shuangtunzi was discharged from a water level of 2500 m through all gates while the upstream Xiazhuang II was breaching. Figure 14 shows the water level. The continuous flooding at Dali needed 8.7 h to propagate to the Shuangtunzi reservoir. At this time, the water level of Shuangtunzi fell to 2493.76 m, where the reduction amplitude was 6.24 m. The flood discharge was still less than that of the outlet structure afterwards, and the water level decreased to the lowest level of 2494.43 m at hour 9.7 when the inflow was equal to the outflow. The flood discharge was subsequently greater than that with all the gates discharging at capacity. The reservoir level started rising until the inflow was equal to the outflow for the second time. The water level rose to its highest at 2507.39 m, which was lower than the crest elevation of 2.61 m. This finding indicated that abnormal flood discharge facilities set in Shuangtunzi based on the original and flood regulation storage capacity increased with pre-warning under the conditions of the upstream class 2 reservoir breach and the mid-stream cascade continuous breach. With flood reg-

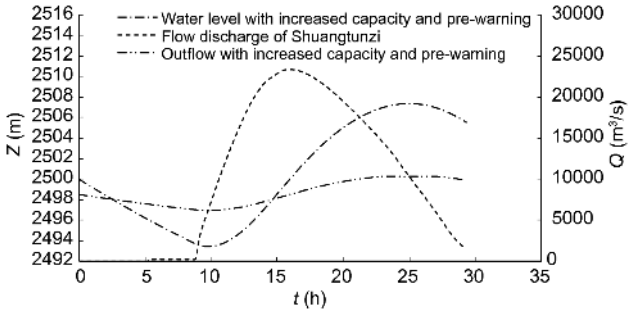

Figure 14 Inflow, outflow, and flood regulation process of Shuangtunzi with an increased discharge capacity and pre-warning for the upstream cascade breaches.

ulation and pre-warning, the final water level margin rose to 2.61 m from 0.21 m, by which time, the safety margin was increased to ensure that the dam would not fail, and the risk of a cascade of continuous breaches was effectively obstructed. Figure 15 summarizes the cascading dam breach process of the abovementioned four cases and the typical breaching characteristic values.

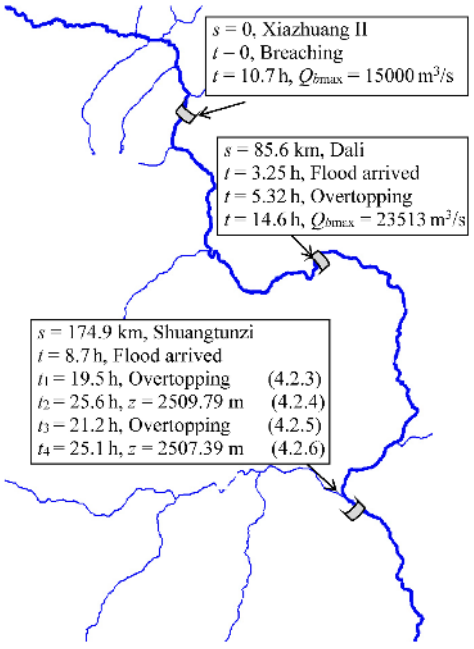

Figure 15 (Color online) Summarized cascading dam breach process of the four cases and the typical breaching characteristic values.

5 Conclusion

This study proposed a platform and a procedure for a numerical simulation of a cascading dam breach for a hazard analysis of cascade reservoirs, including 1D flow modeling of the river channel, flood propagation, regulation process of reservoir fluctuation, overtopping with breaching, and wave damping downstream. A hyperbolic model of the DB-IWHR was embedded into the platform to simulate the dam breaching process. In calculating the cascading dam breach, the propagated flow caused by the overtopping from the initial breach should overlap with the inflow of the reservoir when the water level reaches the dam crest. Five breach models and software were used to calculate the breaching of the Tangjiashan barrier lake. The results showed that the proposed methodology and the continuous breach modeling platform can guide model users in predicting flows generated by dam failures for a cascade of dams.

With the aim of examining the layouts of the watershed cascade cases I and II, the safety problems of the cascade system were investigated from the perspective of the discharge safety of key control cascades and the necessity of increasing the abnormal flood discharge facilities in light of extreme operating conditions. The class 1 dam of case I must enhance the abnormal overflow facilities to better deal with these working conditions. In addition, its initial conditions must be decided according to the failure conditions of the gate and the forecasted or monitored peak discharge and time. For layout case II, if a breach occurred in the upstream special class 2 dam in the presence of a pre-warning, the downstream control cascade class 1 dam was guaranteed protection from the breach. The downstream class 1 dam further lowered the water level before the flooding caused by a breach in the upstream dam reached the reservoir by setting the abnormal flood discharge facilities to increase the margin of the flood discharge. A case study showed that the degree of safety of the downstream class 1 dam clearly improved using these measures. A specific setting-up magnitude and a feasible design approach to increase the discharge capacity were given. The spacing was usually limited to the risk activation cascade and the control cascade; hence, once the upstream cascade is breached, the time of a pre-warning of risk for the control cascade is counted by hour. Therefore, the time of pre-warning of the dam breach is very significant for the control cascade discharge safety when dams are arranged in series.

The soil erosion rate of the model was one of the critical parameters affecting the results (i.e., between 0.4 and 1.1 mm/s). The values were associated with a shear stress range of 20–100 Pa for the abovementioned case given the limited amount of data. However, other rock-filled dams for cohesive and non-cohesive soil materials might have introduced a significant uncertainty in terms of the parameter input. Thus, the soil erosion and shear strength tests should be performed first to calibrate the parameters. A lack of understanding of the dam breach processes leads to further research and more independent tests and observations to validate the model for it to suit the different characteristics of cases of application and reduce the risk of using inappropriate parameters.

This work was supported by the National Key Research and Development Program of China (Grant No. 2016YFC0401706), the National Natural Science Foundation of China (Grant No. 51679262), and the IWHR Research & Development Support Program (Grant Nos. HY0145B642017, and HY0145B802017).

1 Guo X L, Yang K L, Xia Q F, et al. Discharge capacity characteristics of piano key weir (in Chinese). J Hydraul Eng, 2014, 46: 867–882
2 Zhu Y H, Visser P J, Vrijling J K, et al. Experimental investigation on breaching of embankments. Sci China Technol Sci, 2011, 54: 148–155
3 Zhou J P, Wang H, Chen Z Y, et al. Evaluations on the safety design standards for dams with extra height or cascade impacts. Part I: Fundamentals and criteria (in Chinese). J Hydraul Eng, 2015, 46: 505–514
4 Li S Y, Zhou X B, Wang Y J, et al. Study of risk acceptance criteria for dams. Sci China Technol Sci, 2015, 58: 1263–1271
5 Du X H, Li B, Chen Z Y, et al. Evaluations on the safety design standards for dams with extra height or cascade impacts. Part II: Slope stability of embankment dams (in Chinese). J Hydraul Eng, 2015, 46: 640–649
6 ASCE/EWRI Task Committee on Dam/Levee Breach. Earthen embankment breaching. J Hydraul Eng, 2011, 137: 1549–1564
7 Singh V P. Dam Breach Modeling Technology. Dordrecht: Kluwer Academic, 1996
8 Wahl T L. Prediction of embankment dam breach parameters: A literature review and needs assessment. Dam Safety Report. No. DSO-98-004, U.S. Department of the interior, Bureau of Reclamation, Denver, 1998
9 Morris M W, Kortenhaus A, Visser P J, et al. Breaching processes: A state of the art review. FLOODsite Report. T06-06-03, FLOODsite Consortium, 2009
10 Xu Y, Zhang L M. Breaching parameters for earth and rockfill dams. J Geotech Geoenviron Eng, 2009, 135: 1957–1970
11 Cristofano E A. Method of computing erosion rate of failure of earth dams. Technical Report. U.S. Bureau of Reclamation, Denver, 1965
12 Harris G W, Wagner D A. Outflow from Breached Earth Dams. Technical Report. Salt Lake City: University of Utah, 1967
13 Fread D L. BREACH: An erosion model for earthen dam failure (model description and user manual). National Oceanic and Atmospheric Administration, National Weather Service, Silver Spring, 1988
14 Walder J S, O'Connor J E. Methods for predicting peak discharge of floods caused by failure of natural and constructed earthen dams. Water Resour Res, 1997, 33: 2337–2348
15 Liang L, Ni J R, Borthwick A G L, et al. Simulation of dike-break processes in the Yellow River. Sci China Ser E-Technol Sci, 2002, 45: 606–619
16 Wang Z, Bowles D S. Three-dimensional non-cohesive earthen dam breach model. Part 1: Theory and methodology. Adv Water Resources, 2006, 29: 1528–1545
17 Zhang J Y, Li Y, Xuan G X, et al. Overtopping breaching of cohesive homogeneous earth dam with different cohesive strength. Sci China Ser E-Technol Sci, 2009, 52: 3024–3029
18 Chang D S, Zhang L M. Simulation of the erosion process of landslide dams due to overtopping considering variations in soil erodibility along depth. Nat Hazards Earth Syst Sci, 2010, 10: 933–946
19 Erpicum S, Dewals B J, Archambeau P, et al. Dam break flow computation based on an efficient flux vector splitting. J Comput Appl Math, 2010, 234: 2143–2151
20 Wu W. Simplified physically based model of earthen embankment breaching. J Hydraul Eng, 2013, 139: 837–851
21 Brown R J, Rogers D C. BRDAM Users Manual. Denver: U.S. Department of the Interior, Water and Power Resources Service, 1981
22 Singh V P, Scarlatos P D, Collins J G, et al. Breach erosion of earthfill dams (BEED) model. Nat Hazards, 1988, 1: 161–180
23 Zhong Q, Wu W, Chen S, et al. Comparison of simplified physically based dam breach models. Nat Hazards, 2016, 84: 1385–1418
24 Sammen S S, Mohamed T A, Ghazali A H, et al. An evaluation of existent methods for estimation of embankment dam breach parameters. Nat Hazards, 2017, 87: 545–566
25 Sattar A M A. Gene expression models for prediction of dam breach parameters. J Hydroinform, 2014, 16: 550–571
26 Zhang M L, Xu Y Y, Hao Z N, et al. Integrating 1D and 2D hydrodynamic, sediment transport model for dam-break flow using finite volume method. Sci China-Phys Mech Astron, 2014, 57: 774–783
27 Wu W, Marsooli R, He Z. depth-averaged two-dimensional model of unsteady flow and sediment transport due to noncohesive embankment break/breaching. J Hydraul Eng, 2012, 138: 503–516
28 Chen Z, Ma L, Yu S, et al. Back analysis of the draining process of the Tangjiashan Barrier Lake. J Hydraul Eng, 2014, 141: 05014011
29 Zhou X, Chen Z, Yu S, et al. Risk analysis and emergency actions for Hongshiyan barrier lake. Nat Hazards, 2015, 79: 1933–1959
30 Dewals B, Erpicum S, Detrembleur S, et al. Failure of dams arranged in series or in complex. Nat Hazards, 2011, 56: 917–939
31 Fread D L. DAMBRK: The NWS dam break flood forecasting model. Report. National Oceanic and Atmospheric Administration, National Weather Service, Silver Spring, 1984
32 Singh V P, Scarlatos P D. Analysis of gradual earth-dam failure. J Hydraulic Eng, 1988, 114: 21–42
33 Liu N, Chen Z, Zhang J, et al. Draining the Tangjiashan barrier lake. J Hydraul Eng, 2010, 136: 914–923